ADVANCED MATERIALS
www.advmat.de

www.MaterialsViews.com

The Study of Spin-Valley Coupling in Atomically Thin Group VI Transition Metal Dichalcogenides

*Bairen Zhu, Hualing Zeng, Junfeng Dai, and Xiaodong Cui**

In the hunt for ultimately thin electronic devices, atomically thin layers of group VI transition metal dichalcogenides (TMDCs) are recognized as ideal 2D materials after the success of graphene. Monolayer TMDCs feature nonzero but contrasting Berry curvatures and valence-band spin splitting with opposite sign at inequivalent K and K′ valleys located at the corners of the 1st Brillouin zone. These features raise the possibility of manipulating electrons' valley and spin degrees of freedom by optical and electric means, which subsequently makes monolayer TMDCs promising candidates for spintronics and valleytronics applications.

1. Introduction

The family of group VI transition metal dichalcogenides (TMDCs) MX_2 (M = Mo,W; X = S,Se) has a structure of an X–M–X covalently bonded hexagonal quasi-2D network, weakly stacked by weak Van der Waals forces. In each MX_2 monolayer, the unit element of the bulk crystal, each metal atom sits in a trigonal prismatic coordination center, being bound to six chalcogenide ligands, and each chalcogen center is pyramidal, being bound to three metal atoms. In this way, the trigonal prisms are interconnected to give a layered structure, wherein metal atoms are sandwiched between layers of chalcogenide atoms, as shown in **Figure 1**. In each TMDC monolayer the crystal symmetry has D_{3h}^1 and inversion symmetry is explicitly broken. While the bulk crystal has the *2H* stacking order with the space group D_{6h}^4, which is inversion symmetric. Materials in this family have similar band structures as well as physical properties. Bulk TMDCs are semiconductors with an indirect gap located between the top of valence band at the Γ points and the bottom of conduction band in middle of the K and Γ points in its Brillouin zone. Atomically thin MX_2 films including monolayers and multilayers, being chemically inert, present a class of intrinsic 2D semiconductors that are widely regarded as a platform for ultimate electronics. As the bulk thins to monolayers, quantum confinement shapes the band structure from an indirect bandgap to a direct band located at the K points in their Brillouin zone.[1,2] Moreover, the direct bandgap lies in the visible and near infrared range and this makes monolayer TMDCs ideal candidates for optoelectronic applications.

In many non-centrosymmetric semiconductors, inequivalent energy extremas exist in the band structure: so called valleys in their Brillouin zone. TMDCs in the group with a hexagonal lattice have energetically degenerate, but inequivalent, valleys at the K and K′ points in their Brillouin zone. These valleys are situated at the corners of the Brillouin zone and separated by a large momentum space, thought to be robust against scattering by low-energy acoustic phonons and slowly varied deformations. This gives electrons an extra degree of freedom, the so-called valley degree of freedom. One proposes to utilize this valley degree of freedom to manipulate electron quantum states and consequently to realize the operation on information. This is the concept of valley-based electronics, so called valleytronics. The first step toward valleytronics is how we distinguish these energetically degenerate but inequivalent valleys. One proposal is to operate through the valley-dependent Berry curvatures and orbital magnetic moments, if any. The Berry curve is defined as $\Omega = \mathrm{Im}\langle\nabla_k\mu_k| \times |\nabla_k\mu_k\rangle$ where μ_K is the Bloch component of the electron wavefunction $|K\rangle$. The orbital magnetic moment shares the similar form as the Berry curvature: $m(k) = -i\frac{e}{2\hbar}\langle\nabla_k\mu_k| \times [H(k) - \varepsilon(k)]|\nabla_k\mu_k\rangle$ where $H(k)$ is the Bloch Hamiltonian and $\varepsilon(k)$ is the band energy. Both describe the valence electron's characteristics owing to crystal periodic conformation.[3] From a simple symmetry analysis point of view, for a crystal with inversion symmetry, a spatial reversal transformation $\vec{r} \to -\vec{r}$ makes $\Omega(\vec{k}) = \Omega(-\vec{k})$ and $m(\vec{k}) = m(-\vec{k})$. If time-reversal symmetry holds, a time-reversal transformation makes $\Omega(\vec{k}) = -\Omega(-\vec{k})$ and $m(\vec{k}) = -m(-\vec{k})$. If both symmetries hold, Berry curvature and the orbital magnetic moment must be zero over the Brillouin zone. Subsequently crystals that lack inversion symmetry or time-reversal symmetry can be expected to have a nonzero Berry curvature and orbital magnetic moment. One paradigm of the theoretical approach has been established on biased bilayer graphene,

B. Zhu, Prof. X. Cui
Physics Department
The University of Hong Kong
Prokfulam, Hong Kong 999077, China
E-mail: xdcui@hku.hk
Dr. H. Zeng
Department of Physics
The Chinese University of Hong Kong
Shatin, New Territories
Hong Kong 999077, China
Dr. J. Dai
Physics Department
South University of Science and Technology of China
No. 1088, Xueyuan Rd., Xili, Nanshan District, Shenzhen 518055, Guangdong, China

DOI: 10.1002/adma.201305367

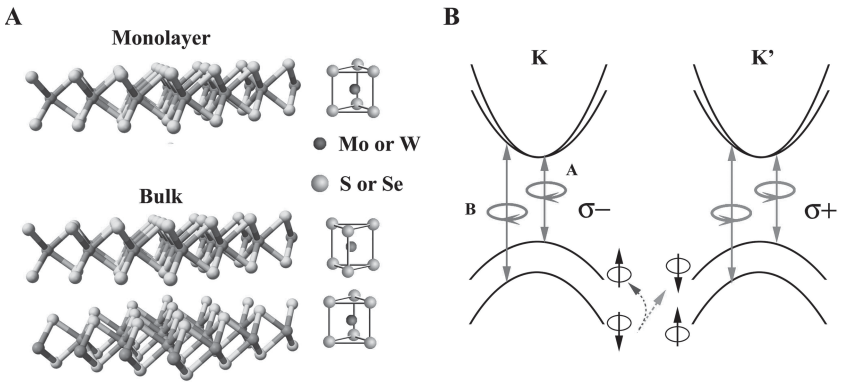

Figure 1. A) Schematics of the MX_2 structure. The unit cell of bulk crystals and even-layer film includes two sub-cells stacking at 2H packing order. B) The valley selective optical selection rules. Nonzero but contrasting Berry curvatures at the K and K′ valleys induce interband circular dichroism: left-handed circularly polarization at the K valley and right-handed at K′. The SOC induces spin splitting of the valence band at the K and K′ valleys. As a result of time-reversal symmetry, spin at the K and K′ valleys points in the opposite direction. Hot carrier relaxation has to go through either a spin flip in the same valley (darker dashed arrow) or intervalley scattering (lighter dashed arrow).

where the structure engineering opens a gap at two inequivalent valleys in the Brillouin zone and breaks the spatial-inversion symmetry.[4] It is predicted that there are nonzero but contrasting Berry curvatures and orbital magnetic moments at the K and K′ valleys in biased bilayer graphene and these contrasting Berry curvatures and orbital magnetic moments could lead to a valley Hall effect, valley selective optical selection rules, etc. [4,5]

Monolayer TMDCs share the similar physics as biased bilayer graphene: the bandgap is located at the K(K′) valley in the Brillouin zone and the inversion symmetry is explicitly broken. It is predicted that there are nonzero but contrasting Berry curvatures and orbital magnetic moments at the K and K′ valleys owing to inversion asymmetry in monolayers.[6] Consequently valley-dependent physics arise in monolayer TMDCs. Moreover, the bandgaps of monolayer TMDCs lie in the and near infrared ranges and this reduces the technique barrier for quantum manipulation with optical fields.

The bottom of the conduction band and the top of the valence band around the K valley are both primarily constructed from metal *d* orbitals that display remarkable spin-orbit coupling(SOC).[7] The spin-orbit coupling splits the valence band by a significant amount, say 0.1–0.2 eV for MoS_2 and around 0.4 eV for WSe_2 and WS_2. As a result of time-reversal symmetry, spin splitting has the opposite sign at the K and K′ valleys. Namely, if the electron spin at the top of valence band is pointing up at the K valley, then the electron spin at the K′ valley must be pointing down. This strong SOC locks the spin and valley degree of freedoms in monolayer TMDCs and offers extra control for quantum manipulations. Furthermore spin-valley coupling suppresses the spin and valley relaxation of the valence electrons, for the spin and valley indices have to be flipped simultaneously. Having the virtues above, monolayer TMDCs are being recognized as an unprecedented platform for valleytronics and spintronics applications.

2. Characterization of Thickness and Inversion Symmetry

Monolayer and multilayer TMDCs can be obtained either by mechanical cleavage from bulk single crystals or by direct growth on substrates by the chemical vapor deposition (CVD) method.[8] Although the present CVD methods can produce large-size single-crystalline monolayer TMDCs, samples exfoliated from bulk single-crystals are still the best option for physics research, owing to the high sample quality. Monolayer and multilayer flakes on top of thin dielectric layers can be visually identified by optical microscopy under bright-field incandescence lumination. The color contrast due to light interference through the sample and thin dielectric layers gives a clear indication of the film thickness. Raman scattering spectroscopy is proven to be a quantitative characterization tool for MoS_2 thickness. Monolayer, bilayer, and multilayer flakes can be identified by the energy difference $\Delta\omega$ between two characteristic Raman modes, the in-plane vibrational E^1_{2g} mode and the out-of-plane vibrational A_{1g} mode: $\Delta\omega$ is around 19 cm^{-1} in monolayer MoS_2 and 21 cm^{-1} in bilayer MoS_2.[9] The thickness dependence of the E^1_{2g} and A_{1g} modes in WX_2 is not significant.[10] In the low-wavenumber range (<50 cm^{-1}), we have also observed two contrasting thickness-dependent Raman modes:[11] shear mode and compression (breathing) modes. With increasing numbers of MoS_2 layers, the shear mode shows a significant increase in frequency, while the compression (breathing) mode decreases following a $1/N$ trend (N denotes the number of layers). The thickness dependence of these two low-frequency modes applies to all MX_2 multilayers.

Inversion symmetry of multilayers and monolayers has been checked by second-harmonic-generation (SHG) experiments.[10] An ultrafast laser beam at 800 nm is incident on multilayer MX_2 and the SHG signal at 400 nm is studied. The SHG signals show a significant even-odd oscillation: a strong SHG is observed for MX_2 multilayers with only an odd unit layer, and the strongest SHG arises from monolayers. The even-layers show little SHG signal. As SHG is determined by the material's second-order susceptibility $\chi^{(2)}$, in the presence of inversion symmetry, $\chi^{(2)}$ must be zero. A dramatic SHG oscillation pattern with an even-odd layer is indeed evidence of the presence (absence) of inversion symmetry in the even-layers (odd-layers). The SHG experiments demonstrate that the multilayer MX_2 follows a $2H$ packing order as in the bulk form.

3. Valley Polarization by Optical Pumping

Valley polarization in monolayer MX_2 can be realized by controlling the polarization of the optical excitation. It is predicted that there is a valley-selective interband optical selection rule around the K(K′) valley in monolayer MX_2 owing to the inversion

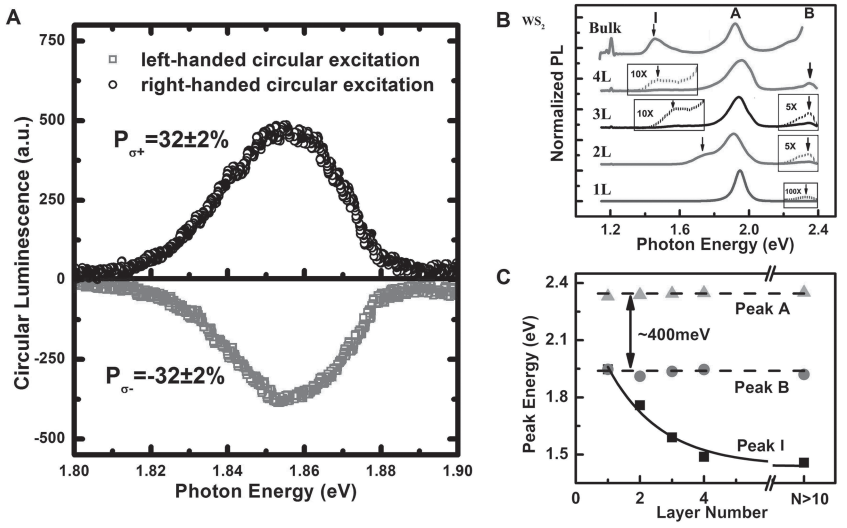

Figure 2. A) Circularly polarized PL of monolayer MoS_2 under circularly polarized excitation at 633nm. Reproduced with permission.[12] Copyright 2012, Nature Publishing Group. B) Photoluminescence spectra of multilayer and monolayer WS_2. "I", "A" and "B" denote PL from indirect bandgap and direct gap transitions from spin-split valence bands respectively. C) The peak position evolution against sample thickness in units of layers. Reproduced with permission.[10] Copyright 2013, the authors; published by Nature Publishing Group.

asymmetry. The interband transitions in the vicinity of the K(K′) point couple exclusively to right (left)-handed circularly polarized light σ+(σ-), as sketched in Figure 1. The direct bandgap transition at the two degenerate valleys together with this valley contrasting selection rules suggest that one can generate and detect valley polarizations in monolayer MX_2 with the polarization of the optical fields. We have demonstrated valley polarization in monolayer MX_2 (MoS_2 and WS_2) by using polarization-sensitive photoluminescence spectroscopy.[12] If the monolayer MoS_2 (WS_2) is excited with circularly polarized light with the near-resonant energy of the band edge, its photoluminescence is circularly polarized and it inherits the helicity of the excitation source, as shown in **Figure 2**. This is the direct consequence of the valley-selective optical selection rules. We have also conducted control experiments to confirm the valley-selective selection rules:[12] i) the polarization of the PL is independent of in-plane magnetic fields up to 0.7 T. This excludes the possibility that the circular polarization arises from the spin-related optical selection rules as in many III–V semiconductors; ii) the PL from bilayer MoS_2 is unpolarized. As the valley-selective optical-selection rules originate from the inversion asymmetry of the monolayer, the selection rule is automatically broken in inversion-symmetric systems (e.g., bilayer MoS_2) where the inversion symmetry is recovered by the 2*H* stacking order.

Besides the prominent PL peak originating from the band edge, the so-called A exciton, a weak peak at the higher energy end (B exciton) also exists, which is attributed to emission from the spin-split valence band as sketched in Figure 1. The energy difference between the two PL peaks implies spin splitting in the valence band owing to the SOC at the K valley, which is around 0.16 eV for monolayer MoS_2 and 0.4 eV for WS_2 and WSe_2. Usually the hot carriers energetically relax to the band edge on a time scale of 10^2–10^4 fs, and the fast decay quenches light emission from the high energy states above the band edge, whereas in TMDCs, the relaxation of the B excitons requires either a spin flip in the same valley or intervalley scattering $K \leftrightarrow K'$ as shown in Figure 1, and neither process is easily satisfied. Consequently the hot-carrier relaxation channel is clogged so that the occurrence of B exciton PL arises.

Remarkably the energy difference between A and B excitons are almost constant at 0.4 eV in WS_2 and WSe_2 multilayers and monolayers.[10] Ab initio calculations show that the giant spin splitting of 0.4 eV in tungsten dichalcogenides tremendously suppresses interlayer hopping at the energy scale of 0.16 eV, whereas the spin splitting is comparable with the interlayer hopping energy in MoS_2. Note that multilayer TMDCs follow a 2*H* packing order: each layer is a 180° in-plane rotation of the adjacent layers. This rotation switches the K and K′ valleys but leaves the spin unchanged, which results in a sign change for the spin-valley coupling from layer to layer. The spin-conserving interlayer hopping at the K and K′ valleys is therefore fully suppressed by the giant spin-valley coupling in tungsten dichalcogenides. A direct consequence is that the splitting patterns remain the same as that of monolayers, and the valence-band Bloch states near the K points are largely localized in individual layers, as if interlayer hopping is absent.[13] The valley-dependent optical-selection rules are valid in direct interband transitions in the K and K′ valleys in WX_2 multilayers.

In this study, we have experimentally demonstrated valley polarization and spin-valley coupling in monolayer and multilayer TMDCs. The spin-valley coupling, with the consequence of spin-valley interplay and the suppression of spin and valley relaxations in TMDCs particularly pronounced in tungsten dichalcogenides, opens a new route toward manipulation of the spin and valley degrees of freedoms. Further experimental investigations of these features are ongoing, facing obstacles in poor sample quality. With fast-growing techniques in the large-scale synthesis of high-quality samples and doping control, in-depth studies of the physics in atomically thin TMDCs, such as spin Hall and valley Hall effects, and interplays of spin and valley degrees of freedoms, are expected, and these studies may guide an unprecedented route towards spintronics and valleytronics.

Acknowledgements

The authors thank Dr. Wang Yao for discussion and Xie Lu, Ruicong He, and Xi Chen for assistance. H.Z. acknowledges financial support from the Direct Grant for Research 2013/2014 in CUHK. This work was supported by the Area of Excellency (AoE/P-04/08) and SRT on New Materials.

Received: October 29, 2013
Revised: January 1, 2014
Published online: April 6, 2014

[1] K. F. Mak, C. Lee, J. Hone, J. Shan, T. F. Heinz, *Phys. Rev. Lett.* **2010**, *105*, 136805.
[2] A. Splendiani, L. Sun, Y. Zhang, T. Li, J. Kim, C.-Y. Chim, G. Galli, F. Wang, *Nano Lett.* **2010**, *10*, 1271.
[3] D. Xiao, M.-C. Chang, Q. Niu, *Rev. Mod. Phys.* **2010**, *82*, 1959.
[4] D. Xiao, W. Yao, Q. Niu, *Phys. Rev. Lett.* **2007**, *99*, 236809.
[5] W. Yao, D. Xiao, Q. Niu, *Phys. Rev. B* **2008**, *77*, 235406.
[6] D. Xiao, G.-B. Liu, W. Feng, X. Xu, W. Yao, *Phys. Rev. Lett.* **2012**, *108*, 196802.
[7] L. F. Mattheiss, *Phys. Rev. B* **1973**, *8*, 3719.
[8] Y.-H. Lee, X.-Q. Zhang, W. Zhang, M.-T. Chang, C.-T. Lin, K.-D. Chang, Y.-C. Yu, J. T.-W. Wang, C.-S. Chang, L.-J. Li, T.-W. Lin, *Adv. Mater.* **2012**, *24*, 2320.
[9] C. Lee, H. Yan, L. E. Brus, T. F. Heinz, J. Hone, S. Ryu, *ACS Nano* **2010**, *4*, 2695.
[10] H. Zeng, G.-B. Liu, J. Dai, Y. Yan, B. Zhu, R. He, L. Xie, S. Xu, X. Chen, W. Yao, X. Cui, *Sci. Rep.* **2013**, *3*, 1608.
[11] H. Zeng, B. Zhu, K. Liu, J. Fan, X. Cui, Q. M. Zhang, *Phys. Rev. B* **2012**, *86*, 241301.
[12] H. Zeng, J. Dai, W. Yao, D. Xiao, X. Cui, *Nat. Nanotechnol.* **2012**, *7*, 490.
[13] Z. Gong, G.-B. Liu, H. Yu, D. Xiao, X. Cui, X. Xu, W. Yao, *Nat. Commun.* **2013**, *4*, 2053.